Available online at www.sciencedirect.com
ScienceDirect
Ceramics International 40 (2014) 3243–3251
CERAMICS INTERNATIONAL
www.elsevier.com/locate/ceramint

Phase transformation behavior of 3 mol% yttria partially-stabilized ZrO_2 (3Y–PSZ) precursor powder by an isothermal method

Chih-Wei Kuo[a], Yun-Hwei Shen[a], Feng-Lin Yen[b,*], Huy-Zu Cheng[c], I-Ming Hung[d], Shaw-Bing Wen[a], Moo-Chin Wang[b,**], Margaret Stack[e]

[a]*Department of Resources Engineering, National Cheng Kung University, 1 Ta-Hsueh Road, Tainan 70101, Taiwan*
[b]*Department of Fragrance and Cosmetics Science, Kaohsiung Medical University, 100 Shih-Chuan 1st Road, Kaohsiung 807, Taiwan*
[c]*Department of Materials Science and Engineering, I-Shou University, 1 Huseh-Cheng Road, Section 1, Ta-Hsu, Kaohsiung 84001, Taiwan*
[d]*Department of Chemical Engineering and Materials Science, Yuan Ze University, No.135, Yuan-Tung Road, Chungli, Taoyuan 320, Taiwan*
[e]*Department of Mechanical and Aerospace Engineering, University of Strathclyde, 75 Montrose Street, Glasgow, UK*

Received 27 August 2013; received in revised form 25 September 2013; accepted 25 September 2013
Available online 3 October 2013

Abstract

The phase transformation behavior of freeze-dried 3 mol% yttria–partially-stabilized zirconia (3Y–PSZ) precursor powder has been studied. When the freeze-dried 3Y–PSZ precursor powder was calcined at 773–1073 K for 2 h, the crystalline structure was composed of tetragonal and monoclinic ZrO_2 as primary and secondary phases, respectively. The freeze-dried 3Y–PSZ precursor powder after calcination at 773 K, the monoclinic ZrO_2 content abruptly increased from 8.00% to 31.51% and the tetragonal ZrO_2 content suddenly decreased from 92.00% to 68.49%, with the duration increasing from 0.5 to 1 min. The activation energy of the isothermal transformation from tetragonal to monoclinic was 7.02 kJ/mol. The kinetics equation for the phase transformation from tetragonal to monoclinic in the freeze-dried 3Y–PSZ precursor powder between 773 K and 1273 K for various durations is described as $\ln(1/1-\alpha)=1/2.61[t^{2.61}(1.50\times10^{-3})^{2.61}\exp(-7.02\times10^{3}/RT)]$; whereas, the HRTEM image shows a typical monoclinic ZrO_2 domain because of the stress-induced tetragonal to monoclinic ZrO_2 martensitic transformation that has occurred.

Keywords: Phase transformation; Tetragonal ZrO_2; Monoclinic ZrO_2; 3 mol% yttria partially stabilized ZrO_2 (3Y–PSZ); Martensitic transformation

1. Introduction

Recently, there have been primary advances in the application of yttria partially-stabilized zirconia (Y–PSZ) ceramics for restorations including fixed partial dentures (FPDs), implant abutments, endodontic posts, resin-bonded FPDs and full-coverage crowns [1,2]. This is because zirconia (ZrO_2) ceramics have a unique combination of mechanical properties such as high wear resistance, low coefficient of fraction and higher crack resistance than alumina and very good biocompatibility [3–6]. The increase in crack resistance is accounted for by its ability to undergo a phase transformation [6–8] from the tetragonal to the monoclinic phase at temperatures from 1443 K to room temperature, accompanied with a volume increase of about 4% but with microcracking as well [6].

The use of pure ZrO_2 as an advance structural material is limited by its spontaneous stress-induced martensitic transformation from tetragonal to monoclinic when going from elaboration temperature to room temperature. The use of 8 mol% Y_2O_3 stabilized ZrO_2 (YSZ) ceramics with a single cubic phase to avoid phase this transformation while going through heating and cooling cycles has reported by Pascual and Duran [9]. When the ZrO_2 contained 3–5 mol% Y_2O_3, the fine-crystallite tetragonal ZrO_2 polycrystals and partially-stabilized ZrO_2 possessed excellent strength and fracture toughness because of the stress-induced martensitic phase transformation from tetragonal to monoclinic.

The retention of the tetragonal phase at room temperature is essential to increase the fracture toughness and fracture strength of partially-stabilized zirconia. Due to its high strength and toughness compared with other ceramics, tetragonal YSZ

---

[*]Corresponding author. Tel: +886 73 121101x2028; fax: +886 73 210683.
[**]Corresponding author. Tel: +886 73 121101x2366; fax: +886 73 210683.
E-mail addresses: flyen@kmu.edu.tw (F.-L. Yen), mcwang@kmu.edu.tw (M.-C. Wang).

0272-8842/$ - see front matter © 2013 Elsevier Ltd and Techna Group S.r.l. All rights reserved.
http://dx.doi.org/10.1016/j.ceramint.2013.09.112

has been regarded as an important engineering ceramic. Moreover, it has been reported that the tetragonal phase on the surface of partially-stabilized zirconia can be rapidly transformed to the monoclinic phase by low-temperature annealing at 473–573 K in air, and both fracture strength and fracture toughness are greatly reduced [10].

Whitney [11] has measured the isothermal transformation rate of a metastable tetragonal to monoclinic ZrO_2 by X-ray diffraction (XRD) using a sample prepared from zirconyl chloride octahydrate by thermal decomposition. Zhu et al. [12,13] have studied the kinetics of 2 mol% and 3 mol% Y_2O_3–ZrO_2 ceramics in the phase transformation from tetragonal to monoclinic and found that this transformation in YSZ ceramics is essentially a time–temperature-transformation curve with a c-shape. These reports show that transformation rate increases with temperature according to Avrami's rate equation, which is based on the nucleation and growth of a new phase [12].

Hsu et al. [14] obtained an activation energy of about 169.2 ± 21.9 kJ/mol for tetragonal ZrO_2 crystallization from freeze-dried 3 mol% yttria stabilized tetragonal zirconia precursor powder using a non-isothermal process. The fraction of monoclinic ZrO_2 content was less than 3.0% when the calcination temperature was below 1073 K, whereas the monoclinic ZrO_2 content increased rapidly to 8.0% when the calcination temperature rose to 1273 K [15]. However, the phase transformation behavior of freeze-dried 3 mol% yttria partially-stabilized ZrO_2 (3Y–PSZ) precursor powder using an isothermal process has not been discussed in detail.

In the present study, using $ZrOCl_2 \cdot 8H_2O$ and $Y(NO_3)_3 \cdot 6H_2O$ as the initial materials, 3Y–PSZ nanocrystallites were synthesized by a coprecipitation process. X-ray diffraction (XRD), transmission electron microscopy (TEM), selected area electron diffraction (SAED), nanobeam electron diffraction (NBED) and high resolution TEM (HRTEM) have been utilized to characterize the phase transformation behavior of the freeze-dried 3Y–PSZ precursor powder by an isothermal method.

The purposes of the present work are to (i) study the phenomenon of phase formation in freeze-dried 3Y–PSZ precursor powder, (ii) research the phase transformation from tetragonal to monoclinic ZrO_2, (iii) research the kinetics of the phase transformation from tetragonal to monoclinic ZrO_2 crystallites and (iv) observe the microstructures of tetragonal and monoclinic ZrO_2 in 3Y–PSZ nanopowder by TEM.

2. Experimental

2.1. Sample preparation

The initial materials were zirconyl chloride ($ZrOCl_2 \cdot 8H_2O$, purity≧99.5%, supplied by Riedel-de Haën, Germany) and yttrium nitrate [$Y(NO_3)_3 \cdot 6H_2O$, purity≧99.5%, supplied by Alfa, United Kingdom]. Zirconyl chloride and yttrium nitrate were dissolved in deionized water and ethanol solution at a ratio of 1:5 vol/vol. Solutions were prepared with Y_2O_3 and ($Y_2O_3+ZrO_2$) in a ratio of 0.03 and labeled as 3Y–PSZ. The mixed solution was then mixed with 1.0 wt% of polyethylene glycol (PEG, extra pure reagent, molecular weight 2000 Da, supplied by Nippon Shyiaku, Kogyo K.K., Japan) as a dispersant because an appropriate amount of PEG can greatly decrease agglomeration. The mixed solution was stirred and heated in a thermostatic bath and held at 348 K for 2 h to obtain a white precipitate. NH_4OH was then added into the solution until pH 9 was attained. After precipitation, the precipitate was repeatedly rinsed and filtered with a large amount of deionized water and tested with $AgNO_3$ solution to make sure no AgCl precipitation occurred. Subsequently, the precipitates were freeze-dried at 218 K in a vacuum. Finally, the freeze-dried precursor powder was heated in a furnace at various temperatures for different durations.

2.2. Sample characterization

The crystalline phase was identified by X-ray diffraction (XRD, Model Rad II A, Rigaku, Tokyo). XRD was performed using an X-ray diffractometer with CuK_α radiation and a Ni filter, operating at 30 kV, 20 mA and a scanning rate (2θ) of 0.25 deg/min. The line broadening method was used to determine the crystallite size of the powder using the Scherrer equation [16]

$$d_{XRD} = \frac{0.89\lambda}{B_{hkl} \cos \theta} \tag{1}$$

where d_{XRD} is the crystallite size, B_{hkl} is the calibrated width of the diffraction peak measured at half maximum intensity, λ is the wavelength of the X-ray radiation and θ is the Bragg angle.

The microstructure of the calcined 3Y–PSZ nanocrystallite powder was examined by transmission electron microscopy (TEM, JEOL, JEM 2100F, Tokyo, Japan) operating at 200 kV. Selected area electron diffraction (SAED) and nanobeam electron diffraction (NBED) were utilized to identify the structure of the 3Y–PSZ nanocrystallites, and a high resolution TEM (HRTEM) examination of the calcined sample was also made.

3. Results and discussion

3.1. Phase formation of freeze-dried 3Y–PSZ precursor powder after calcination at various temperatures for 2 h

Fig. 1 illustrates the XRD patterns of the freeze-dried 3Y–PSZ precursor powder calcined at various temperatures for 2 h. The XRD pattern of the freeze-dried 3Y–PSZ precursor powder calcined at 773 K for 2 h is illustrated in Fig. 1(a). It reveals that the crystalline phase of tetragonal ZrO_2 has appeared. In addition, the broadening reflection peaks of Fig. 1(a) reveal either the poor crystallinity of the tetragonal ZrO_2 and/or it is composed of small crystallites in the submicron to nanometric range [17,18]. Fig. 1(b) shows the XRD pattern of the freeze-dried 3Y–PSZ precursor powder calcined at 873 K for 2 h, which reveal that the monoclinic peaks of $(\bar{1}11)_M$ and $(111)_M$ has also appeared. The reflection peak of $(111)_M$ is very weak and broad, indicating poor crystallinity and/or small crystallite size [17,18]. Moreover,

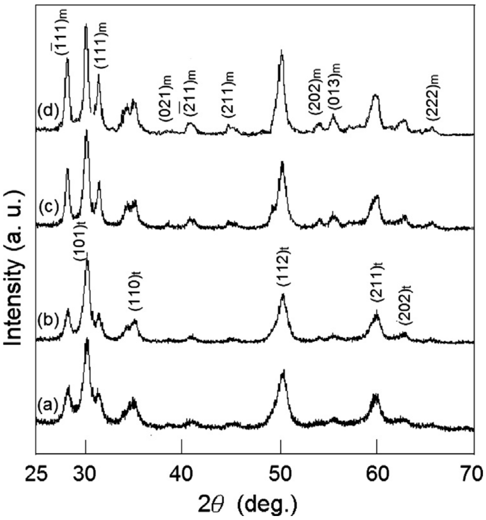

Fig. 1. XRD patterns of freeze-dried 3Y–PSZ precursor powder calcined at different temperatures for 2 h: (a) 773 K, (b) 873 K, (c) 973 K and (d) 1073 K.

the crystallinity of the tetragonal phase in Fig. 1(b) has suddenly increased beyond that shown in Fig. 1(a). Freeze-dried 3Y–PSZ precursor powder calcined at 973 and 1073 K for 2 h are shown in Fig. 1(c) and (d). It can be seen that the monoclinic and tetragonal phases coexist and that the intensity of the reflection peaks is greater than the corresponding peak shown in Fig. 1(b). The intensity of the monoclinic peaks $(\bar{1}11)_M$ and $(111)_M$ increases when the calcination temperature is raised from 973 to 1073 K. Moreover, the crystallinity and crystallite size of the tetragonal phase are also remarkably improved. This occurred because the crystallinity and size of the tetragonal ZrO_2 increased with the rising calcination temperature.

The transformation from low-temperature tetragonal ZrO_2 to monoclinic ZrO_2 in the hydrous zirconia system is particularly rapid between 773 and 873 K, according to Whitney [11]. Gorman and Stubican [19] also demonstrated that the phase equilibrium in the zirconia-rich part of the $ZrO_2-Yb_2O_3-Y_2O_3$ system was determined at 1473, 1673 and 1923 K. The stabilizing effects of Yb_2O_3 and Y_2O_3 were found to be quite similar, with less than 10 mol% of either being necessary to fully stabilize the cubic fluorite-structure phase at 1473 K. The two binary ordered phases, $Zr_3Yb_4O_{12}$ and $Zr_3Y_4O_{12}$, are completely miscible at 1473 K. In the present study, the optimal Y_2O_3 and maximum calcination temperature are only 3 mol% and 1073 K, respectively. Hence, cubic ZrO_2 and the ordered phase of $Zr_3Y_4O_{12}$ are not found.

Moreover, in a $ZrO_2-Y_2O_3$ system, spontaneous transformation from the metastable cubic phase to the tetragonal phase can be triggered at room temperature by a mechanical force. The fact that tetragonality decreases with the addition of Y_2O_3 and vanishes at 9 mol% Y_2O_3 has also been demonstrated by Sheu et al. [20]. In addition, the phase is maintained in the glassy state when the 3Y–PSZ precipitates are calcined at 623 K for 2 h [18]. Their tetragonality decreased as the calcination temperature increased. This result is due to the fact that the mechanical force in the freeze-dried 3Y–PSZ precursor powder is very low and tetragonal is not triggered by the phase transformation. On the other hand, the phase transformation of freeze-dried 3Y–PSZ precursor powder calcined at 673–1073 K for 2 h occurred can be attributed to the tetragonal phase triggered in zirconia solution. Zr has its own characteristic local structure which is dopant-independent but phase-dependent [21].

Table 1
The crystallite size of tetragonal ZrO_2 for 3Y–PSZ precursor powders after calcinations at various temperatures for different durations.

Crystallite size (nm) Temp. (K)	Durations (min)					
	10	20	30	60	90	120
773	9.05	9.42	9.71	10.29	10.48	10.73
873	11.12	11.33	11.62	12.29	12.67	12.85
973	13.57	13.71	14.00	14.67	14.92	15.36
1073	15.62	15.81	16.27	17.52	17.90	18.30

3.2. Isothermal phase transformation of tetragonal to monoclinic ZrO_2 when the freeze-dried 3Y–PSZ precursor powder after calcination

The crystallite sizes of tetragonal ZrO_2 for 3Y–PSZ precursor powders after calcination at various temperatures for different durations are listed in Table 1. It is seen that the crystallite size only increases slightly from 9.05 nm to 10.73 nm when calcined at 773 K for 10–120 min. In contrast, the crystallite size of tetragonal ZrO_2 undergoes an obvious increase when the calcinations temperature is greater than 973 K.

Table 1 also reveals that the crystallite size of tetragonal ZrO_2 are 9.05 nm and 11.12 nm when the 3Y–PSZ precursor powders after calcination at 773 K and 873 K for 10 min, respectively. These results show that the crystallite growth is very slow when calcinations temperature is lower than 873 K. The crystallite size then rapidly increases from 15.62 nm to 17.52 nm when calcined at 1073 K for 10–60 min. Subsequently, the crystallite size only increases slightly from 17.52 nm to 18.30 nm when calcined at 1073 K for 60–120 min, respectively.

The dependence of the relative crystallinity of the tetragonal ZrO_2 on the calcination temperature is illustrated in Fig. 2. Igawa et al. [22] demonstrated that the rate of phase transformation from the metastable tetragonal to the monoclinic phase of ZrO_2 increases with temperature. The tetragonal ZrO_2 in the freeze-dried 3Y–PSZ precursor powder underwent a gradual increase in integrated intensity and crystallinity with increasing calcination temperature and time, indicating that higher calcination temperature and longer time enhance the crystal growth of tetragonal ZrO_2.

The phase content of tetragonal (α_T) and monoclinic (α_M) can be calculated using the intensity of the reflection hkl in the X-ray powder diffraction pattern from the surface of a thick slab of the crystal powder, as proposed by Butler [23]. When the phase transforms from tetragonal to monoclinic, the ratios

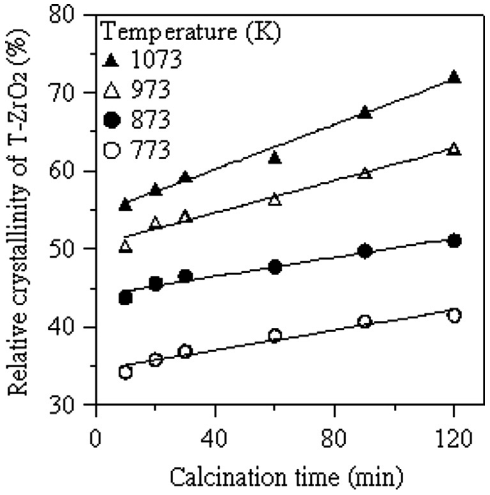

Fig. 2. The relative crystallinity of tetragonal ZrO_2 in freeze-dried 3Y–PSZ precursor powder calcined at various temperatures and durations.

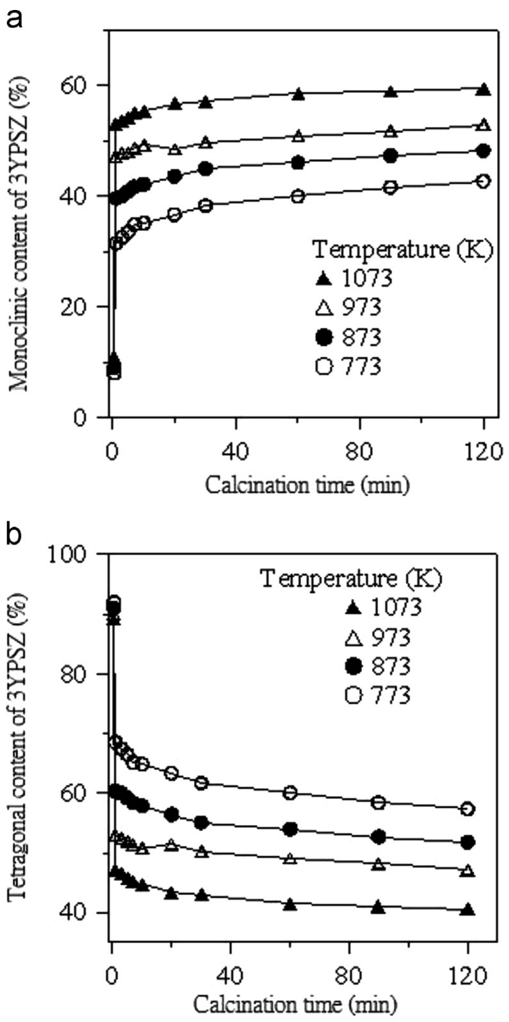

Fig. 3. Relation between the fraction of (a) monoclinic ZrO_2 and (b) tetragonal ZrO_2 and calcination time for freeze-dried 3Y–PSZ precursor powder after being calcined at various temperatures and times.

of the tetragonal and monoclinic phases are defined by

$$\alpha_T(\%) = [I_T(1\ 1\ 1)]/[I_M(\bar{1}\ 1\ 1)+I_M(1\ 1\ 1)+I_T(1\ 1\ 1)] \qquad (2)$$

and,

$$\alpha_M(\%) = [I_M(\bar{1}\ 1\ 1)+I_M(1\ 1\ 1)]/[I_M(\bar{1}\ 1\ 1)+I_M(1\ 1\ 1)+I_T(111)] \qquad (3)$$

where α_T is the ratio of the tetragonal phase, α_M is the ratio of the monoclinic phase, and I_T and I_M are the intensities of the tetragonal and monoclinic phases, respectively.

As shown in Fig. 3, when the freeze-dried 3Y–PSZ precursor powder was calcined at 773 K, the content of monoclinic ZrO_2 abruptly increases from 8.00% to 31.51% (Fig. 3(a)) and tetragonal ZrO_2 suddenly decreases from 92.00% to 68.49% (Fig. 3(b)) as the holding time increases from 0.5 to 1 min. The monoclinic ZrO_2 content increases slightly from 35.10% to 42.71% when the 3Y–PSZ precursor powders after calcination at 773 K from 10 to 120 min. The tetragonal ZrO_2 decreases when the calcination temperature is raised from 773 to 1073 K as shown in Fig. 3(b).

The necessary and sufficient conditions for classifying a transformation as martensitic are that it is “a first-order, solid state structural change which is displacive, diffusionless, and dominated in its kinetics and morphology by the strain energy arising from shear or shear-like displacements” [24]. The first-order character of the transformation implies the coexistence of the parent and product phases at an intermediate stage of transformation, and therefore the existence of an interface. In a martensitic type of transformation, strain centers serve as nucleation sites for the new phase. The platelike nuclei grow very rapidly until they encounter neighboring plates or other constraints. Therefore, a large amount of transformation occurs suddenly under appropriate conditions [25]. The tetragonal–monoclinic transformation in ZrO_2 is known to be martensitic. The clear demonstration that the metastable tetragonal phase can be retained at temperatures well below the equilibrium transformation temperature has important consequence. When heated above a certain critical temperature, powder samples with a high tetragonal phase content abruptly shift to the monoclinic phase upon cooling. As shown in Fig. 3, at the various calcination temperatures for 0.5 min, the tetragonal phase ZrO_2 contents are close to about 90%. Only 68.5% tetragonal phase ZrO_2 is obtained when calcined at 773 K for 1 min; as the calcination temperature is raised to 1073 K, there is an abrupt decrease in tetragonal phase ZrO_2 upon cooling and a corresponding increase in monoclinic phase ZrO_2. This behavior is believed to be caused by the change in crystallite size [26,27]. Crystallite growth appears to either trigger a transformation or provide active nucleation sites [28] for phase transformation. Moreover, Subbaro et al. [26] also pointed out that the monoclinic–tetragonal transformation is one in which some atoms move a significant distance while other atoms retain nearly their original positions. The high-temperature phase is non-quenchable, well-crystallized materials exhibit thermal kinetics and small crystallites undergo isothermal transformation.

In the present study, the crystallite size of tetragonal ZrO_2 increases from 9.05 nm to 15.62 nm when calcined at 773–1073 K for 10 min, respectively. On the other hand, the phase

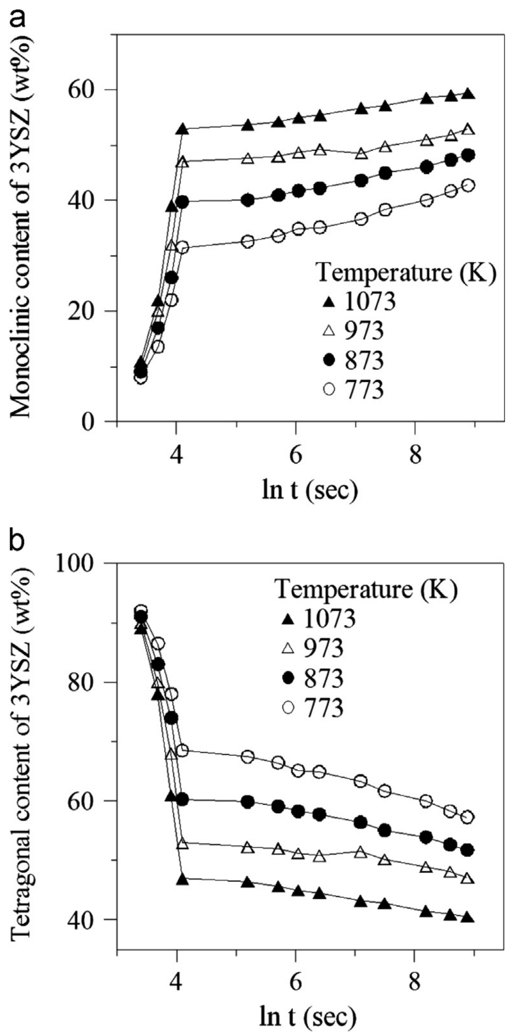

Fig. 4. Plot of (a) monoclinic ZrO_2 and (b) tetragonal ZrO_2 content versus ln *t* of Fig. 3.

content of tetragonal ZrO_2 decreases from 68.49% to 46.50% when calcined at 773–1073 K for 1 min, respectively. When calcination duration prolongs from 20 min to 120 min, only little change for tetragonal ZrO_2 content. According to these results, it is seen that the tetragonal suddenly transformed to monoclinic when calcined at 773–1073 K at initial period of duration due to the strain energy raising from shear or shear-like displacements increased with crystallite size growth [24]. Moreover, the amount of tetragonal transformation to monoclinic ZrO_2 increased with increasing crystallite size [29]. When the calcinations durations increase from 20 min to 120 min, the phase content only little changes because for any phase transformation of solid state associated with an endothermic effect when heating materials with the phase stability, the crystallite size of the materials must be smaller than that of a critical sizes [30]. In the present study, the crystallite size of tetragonal ZrO_2 is smaller than that of 20 nm when calcined at 1073 K for 120 min. This value is also much smaller than that of 30 nm [31].

The powder showed a continuous decrease in the tetragonal phase (with corresponding increasing in monoclinic phase) with increasing temperatures and times. As shown in Fig. 3, the higher the temperature and longer the time, the greater the conversion upon cooling. The free particles have a larger surface area compared to those of crystallites located inside the disc, or even at the outer surface of the disc. Inspection of Fig. 3, further indicates that the phase transformation in the powder is a kinetic process with a dependence on temperature and time [27].

The pressure dependence of the temperature of the reversible phase transformation for tetragonal to monoclinic in zirconium oxide agrees with the slope of the pressure-temperature equilibrium curve up to 15 kbar as calculated from thermodynamics, i.e. $dT/dp = -3.02 \times 10^{-2}$ deg/bar as reported by Whitney [32]. But in the present study, the precipitates and calcined product of ZrO_2 were under atmosphere. Hence, the tetragonal–monoclinic transformation in ZrO_2 is independent of pressure, but dependent on a number of other factors, e.g. calcination temperature, time and initial crystallite, etc.

It has been suggested that the crystallization of pure tetragonal zirconia could be considered as a nucleation and growth process [33], whereby plotting the fraction of

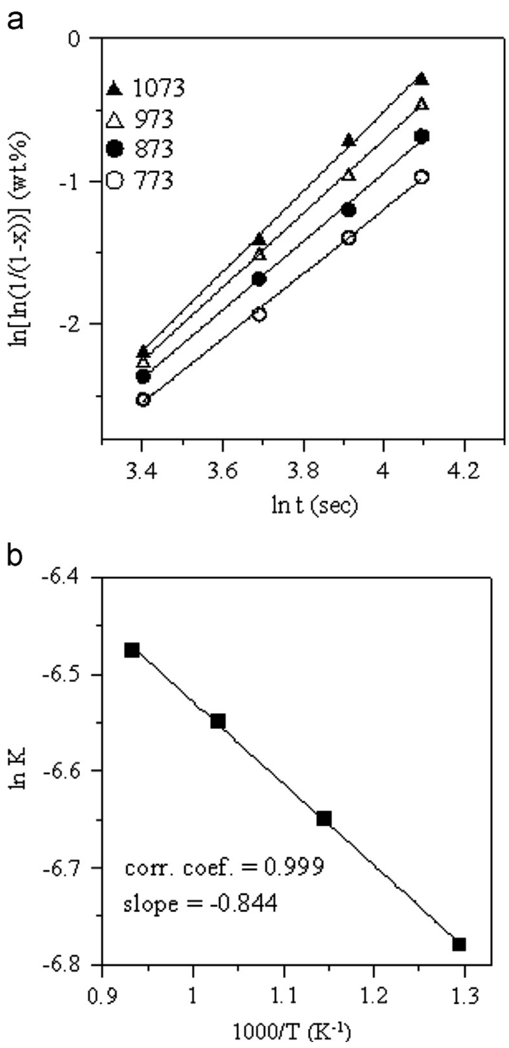

Fig. 5. (a) The relationship between $\ln\left[\ln(1/1-\alpha)\right]$ and ln *t*, and (b) Plot of ln *k* versus 1/*T* for freeze-dried 3Y –PSZ precursor powder at various temperatures.

crystallized monoclinic phase as a function of log time would lead to a sigmoidal curve that should be in close agreement with the Avrami model [34] where crystal growth is assumed to be controlled by nucleation.

Fig. 4 shows the relation between (a) monoclinic ZrO_2 content, (b) tetragonal ZrO_2 content and the nature logarithm ($\ln t$) of calcination time. It can be seen that the relation between monoclinic ZrO_2 content and $\ln t$ exhibited a *C*-curve trend. This result is due to the rapid growth in monoclinic ZrO_2 after the nucleation period. Therefore, the curve in Fig. 4(a) can be suggested to represent the crystallization of monoclinic ZrO_2 controlled by nucleation and growth [34].

3.3. Phase transformation kinetics from tetragonal to monoclinic in freeze-dried 3Y–PSZ precursor powder after calcination

The formation of monoclinic ZrO_2 detected by XRD in the freeze-dried 3Y–PSZ precursor powder is shown in Fig. 3(a). The fraction existing as monoclinic ZrO_2 is a function of calcination temperature and time. To obtain the kinetic parameters for the crystallization of the monoclinic ZrO_2, the following rate equation is assumed [35]:

$$\frac{d\alpha}{dt} = k^n t^{n-1}(1-\alpha), \tag{4}$$

where α is the fraction of monoclinic ZrO_2 as a function of time t, n is a constant dependent on the nucleation and growth mechanism (growth morphology parameter), and k is the rate constant. The exponent n is not only characteristic of the nucleation and growth, but also strongly depends on the kinetic features (mainly nucleation and growth speed).

Table 2
Rate constant (k) and growth morphology parameter (n) for freeze-dried 3Y–PSZ precursor powder.

Calcined temperature (K)	Rate constant (sec^{-1})	Average rate constant (sec^{-1})	Growth morphology parameter (n)	Average growth morphology parameter
773	1.14×10^{-3}	1.35×10^{-3}	2.37	2.61
873	1.30×10^{-3}		2.49	
973	1.43×10^{-3}		2.68	
1073	1.54×10^{-3}		2.89	

The integrated form of Eq. (4) can be expressed by the well-known Johnson–Mehl–Avrami (JMA) equation [34,36]

$$\ln\left(\frac{1}{1-\alpha}\right) = \frac{1}{n}(kt)^n \tag{5}$$

Eq. (6) is obtained by taking the logs of both sides of Eq. (5). For an isothermal process, the experimental data can be better fitted according to the following linear Eq. (6)

$$\ln\ln\left(\frac{1}{1-\alpha}\right) = n\ln k + n\ln t - \ln n \tag{6}$$

A plot of $[\ln\ln(1/(1-\alpha))]$ as a function of $\ln t$ yields the values of n and k shown in Fig. 5. From Eq. (6) and Fig. 5(a), the growth morphology parameter n is obtained and listed in Table 2. The temperature dependence of k in Eq. (4) apparently follows an Arrhenius relationship, according to:

$$k = A\exp\left(-\frac{E_T}{RT}\right), \tag{7}$$

where A is the frequency factor, E_T is the apparent activation energy for the isothermal transformation from tetragonal to monoclinic, and R is the gas constant.

A plot of $\ln k$ versus $1/T$ yields a straight line with a very good correlation coefficient (>0.999), as shown in Fig. 5(b). A straight line is obtained, and then the apparent activation energy of the isothermal transformation from the tetragonal to the monoclinic phase can be calculated from its slope, namely 7.02 kJ/mol.

The kinetic equation for the phase transformation from tetragonal ZrO_2 to monoclinic ZrO_2 in the freeze-dried 3Y–PSZ precursor powder is thus described as

$$\ln\left(\frac{1}{1-\alpha}\right) = \frac{1}{2.61}\left[t^{2.61}\cdot(1.50\times10^{-3})^{2.61}\exp\left(-\frac{7.02\times10^3}{RT}\right)\right]$$

$$\text{for } 773\text{ K} \le t \le 1073\text{ K} \tag{8}$$

The activation energy of 106 kJ/mol was obtained for isothermal tetragonal-to-monoclinic transformation of a 3Y–TZP ceramic at 343–403 K has reported by Chevalier et al. [37]. They demonstrated that the nucleation and growth to be key mechanism for transformation due to the variation of the monoclinic fraction with time for all temperatures. The

Table 3
Activation energy for the isothermal phase transformation from tetragonal to monoclinic ZrO_2 for different types of precursors.

Process	Materials	Method		Activation energy (kJ/mol)	Refs.
Sintering at 1673 K at 1873 K for 5 h	2 mol% yttria-doped zirconia	Isothermal	Transformation (t→m)	41.52 18.67	[12]
Sintering at 1873 K for 5 h	3 mol% yttria-doped zirconia	Isothermal	Transformation (t→m)	22.74	[13]
Co-precipitation	3Y–TZP	Isothermal	Transformation (t→m)	100	[37]
Hot pressed at 1873 K under 25 MPa for 1 h	2 mol% yttria-doped zirconia	isothermal	Nucleation and growth of new phase	28.67	[39]
	5 wt% yttria-stabilized zirconia	Isothermal	Transformation kinetics	~70	[40]
Co-precipitation	3 mol% yttria-doped zirconia	Isothermal	Transformation kinetic (t→m)	7.02	This study

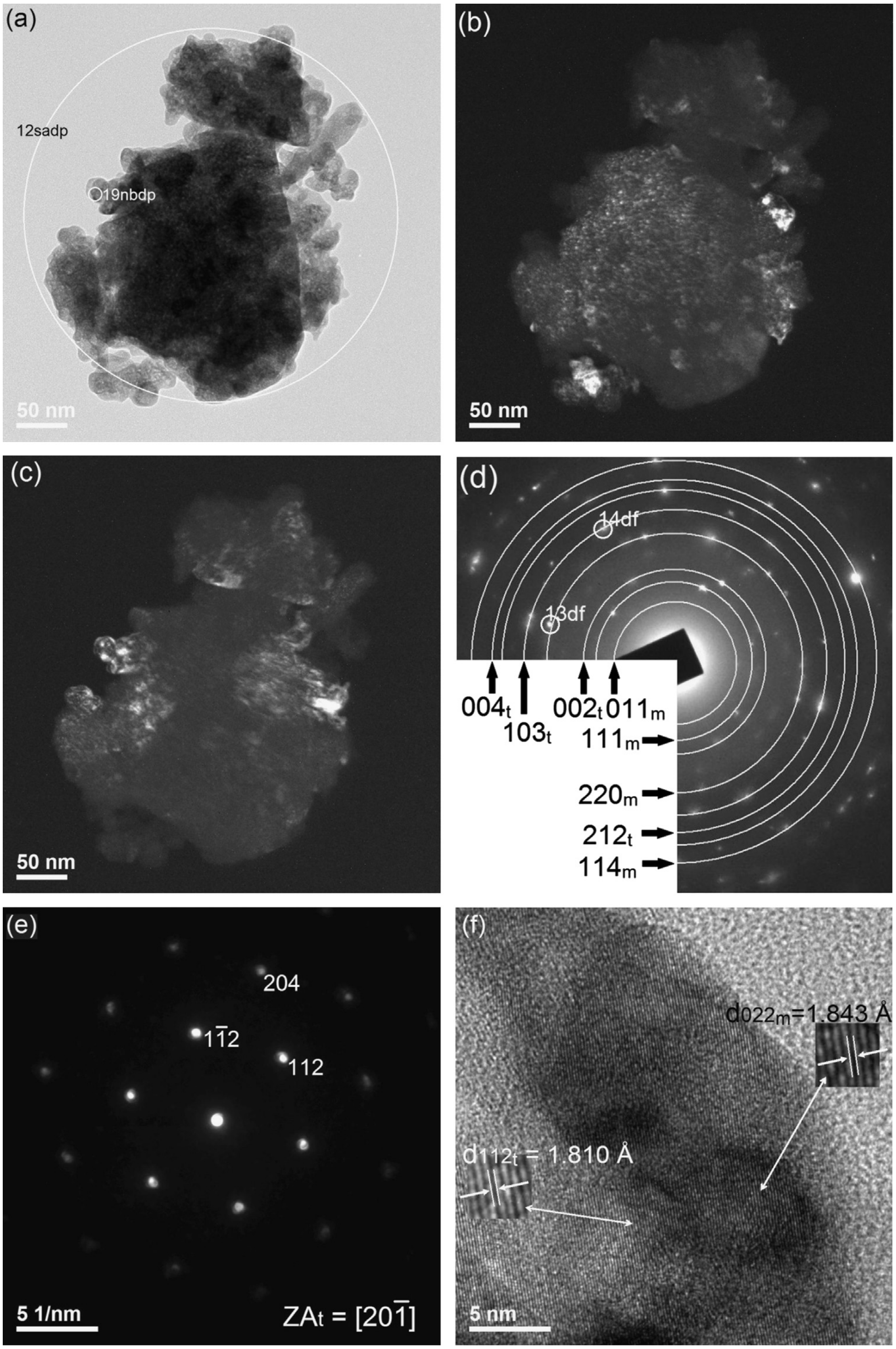

Fig. 6. TEM and HRTEM micrographs of freeze-dried 3Y–PSZ precursor powder calcined at 773 K for 2 h: (a) BF image, (b) DF image using the circle denoted by "13df" in Fig. 6(d), (c) DF image using the circle denoted by "14df" in (d), (d) SAED pattern in the location denoted by "12sadp" in Fig. 6(a) which was indexed as corresponding to the coexistence of monoclinic and tetragonal ZrO_2 phases, and (e) NBED pattern of location denoted by "19nbdp" in Fig. 6(a) which was indexed as corresponding to monoclinic ZrO_2 with ZA = [20$\bar{1}$], and (f) HRTEM image showing the d-spacings of monoclinic ZrO_2 (022) (denoted by 022_m) and tetragonal ZrO_2 (112) (denoted by 112_t) reflections are 1.843 Å and 1.810 Å, respectively.

activation energy of 7.20 kJ/mol for the isothermal transformation from tetragonal to monoclinic ZrO_2 is much less than the reported values of 18.67 kJ/mol and 41.52 kJ/mol for 2YSZ at 1873 and 1673 K, respectively [12]. This indicates that the smaller the crystallite size the larger the value, and consequently the smaller the transformation rate [12]. The result is due to the fact that tetragonal ZrO_2 nanopowder can easily attain a critical nuclei size and then be subsequently transformed to monoclinic ZrO_2. Moreover, Whitney [11] measured the isothermal of metastable tetragonal ZrO_2 to the monoclinic phase by thermal decomposition of precursors have pointed out that the phase transformation rate increased with temperature according to Avramis rate equation [34], which was based on the nucleation and growth of a new phase. Moreover, the crystallite growth–martensite transformation model of tetragonal to monoclinic phase transition also reported by Murakami and Ohno [38], and Igawa et al. [22]. Zhu and Yan [12] also pointed out that transformation rate depends on activation energy was large and starting temperature for tetragonal transformation into monoclinic ZrO_2 was high when crystallite size was large, which leads to a larger growth velocity. On the other hand, when crystallite size was small, although incubation period was short, the transformation rate thereafter was small. Whereas, when the crystallite size was large, although incubation period was long but the transformation rate thereafter was large which results in large volume fraction of isothermal monoclinic phase formed. Therefore, the transformation rate depends on activation energy for transformation. The activation energies of the isothermal transformation from the tetragonal to the monoclinic phase for various precursors and with calcination at different temperatures are listed in Table 3 [12,13,37,39,40].

Eq. (6) and Fig. 5(a) indicate that the isothermal growth morphology parameter n is approximately 3. The parameter $n=3$ in the JMA equation corresponds to diffusion-controlled spherical growth from a constant number of nuclei [34,41,42]. The TEM micrographs in Fig. 6 show that spherical crystals are formed in the 3Y–PSZ powder, supporting the analytical result that crystals grow in the form of near spheres.

3.4. Microstructure of the 3Y–PSZ nanocrystallites

The bright and dark field (BF and DF) TEM micrographs of the freeze-dried 3Y–PSZ precursor powder calcined at 773 K for 2 h are shown in Fig. 6. The ZrO_2 nanocrystallites appear as dark particles with a diameter ranging from 15 to 20 nm as shown in Fig. 6(a). Fig. 6(b) shows the DF image using the circle denoted by “13df” in Fig. 6(d), which reveals the monoclinic ZrO_2 nanocrystallites. Fig. 6(c) shows the DF image using the circle denoted by “14df” in Fig. 6(d), which reveals the tetragonal ZrO_2 nanocrystallites. Fig. 6(d) shows the SAED pattern of location area denoted by “12sadp” in Fig. 6(a), which corresponds to the coexistence of monoclinic and tetragonal ZrO_2. Fig. 6(e) shows the NBED pattern of location denoted by “19nbdp” in Fig. 6(a), which corresponds to the tetragonal ZrO_2 with zone axes of $[20\bar{1}]$. Fig. 6(f) shows a HRTEM image; the d-spacings of monoclinic ZrO_2 (022) and tetragonal ZrO_2 (112) reflections were found to be 1.843 Å and 1.810 Å, respectively.

These results also provide evidence for the coexistence of monoclinic and tetragonal ZrO_2. Monoclinic ZrO_2, which occurs extensively, shows the typical microstructure because of the stress-induced tetragonal to monoclinic ZrO_2 martensitic transformation. The preexisting monoclinic domains may well act as heterogeneous nuclei for tetragonal to monoclinic transformation. Therefore, if the tetragonal ZrO_2 nanocrystallite is only metastable, thermal treatment of the ground powder should lead to complete transformation into the monoclinic structure. On the other hand, if the unstrained tetragonal ZrO_2 nanocrystallites are indeed thermodynamically more stable than monoclinic ZrO_2, one would expect the crystal structure to revert back to tetragonal ZrO_2 once sufficient thermal energy is supplied to remove the stress and strain [43].

4. Conclusion

The phase transformation behavior of tetragonal to monoclinic ZrO_2 in a freeze-dried precursor powder of 3 mol% yttria partially-stabilized zirconia (3Y–PSZ) has been investigated by an isothermal method. The conclusions are as follows:

(i) The crystalline structure is composed of tetragonal ZrO_2 (t-ZrO_2) and monoclinic ZrO_2 (m-ZrO_2) as the primary and secondary phases, respectively, when the freeze-dried 3Y–PSZ precursor powder is calcined between 773 K and 1073 K for 2 h.

(ii) When calcined from 773 to 1073 K, the crystallinity of the freeze-dried 3Y–PSZ precursor powder increases with rising calcination temperature and time. After the freeze-dried 3Y–PSZ precursor powder is calcined at 773 K for 120 min, the tetragonal ZrO_2 and monoclinic ZrO_2 contents are 57.49% and 42.71%, respectively.

(iii) The activation energy for the isothermal transformation of tetragonal ZrO_2 to monoclinic ZrO_2 is 7.02 kJ/mol when the freeze-dried 3Y–PSZ precursor powder is calcined between 773 K and 1073 K for 2 h.

(iv) When the freeze-dried 3Y–PSZ precursor powder was calcined between 773 K and 1073 K, the kinetic equation for phase transformation from tetragonal ZrO_2 to monoclinic ZrO_2 is described by

$$\ln\left(\frac{1}{1-\alpha}\right)=\frac{1}{2.61}\left[(1.50\times10^{-3}t)^{2.61}\exp\left(-\frac{7.02\times10^{3}}{RT}\right)\right],$$

where α is the fraction of monoclinic ZrO_2 as a function of time t.

(v) An HRTEM image shows the typical microstructure resulting from the stress-induced tetragonal to monoclinic ZrO_2 martensitic transformation.

Acknowledgments

The authors gratefully acknowledge the financial support of the Ministry of Economic Affairs, Taiwan, Republic of China, under Grant 102-EC-17-A-08-S1-142, and also deeply thank Prof. M.H. Hon and Mr. S.Y. Yau for offering valuable advice and suggestions on the experiments and analyses.

References

[1] B. Yang, H.C. Lange-Jansen, M. Scharnberg, S. Wolfart, K. Ludwig, R. Adelung, M. Kern, Influence of saliva contamination on zirconia ceramic bonding, Dental Materials 24 (2008) 508–513.

[2] T. Kosmač, Č. Oblak, L. Marion, The effects of dental grinding and sandblasting on ageing and fatigue behavior of dental zirconia (Y-TZP) ceramics, Journal of the European Ceramic Society 28 (2008) 1085–1090.

[3] J.R. Kelly, Ceramics in restorative and prosthetic dentistry[1], Annual Review of Materials Science 27 (1997) 443–468.

[4] A. Wohlwend, S. Studer, P. Schärer, The zirconium oxide abutment: an all-ceramic abutment for the esthetic improvement of implant superstructures, Quintessence of Dental Technology 1 (1997) 63–74.

[5] C. Piconi, G. Maccauro, Zirconia as a ceramic biomaterial, Biomaterials 20 (1999) 1–25.

[6] S. Deville, J. Chevalier, G. Fantozzi, J.F. Bartolomé, J. Requena, J.S. Moya, R. Torrecillas, L.A. Díag., Low-temperature ageing of zirconia-toughened alumina ceramics and its implication in biomedical implants, Journal of the European Ceramic Society 23 (2003) 2975–2982.

[7] A.H. Heuer, Transformation toughening in ZrO_2-containing ceramics, Journal of the American Ceramic Society 70 (1987) 689–698.

[8] R.H.J. Hannink, P.M. Kelly, B.C. Muddle, Transformation toughening in zirconia-containing ceramics, Journal of the American Ceramic Society 83 (2000) 461–487.

[9] C. Pascual, P. Duran, Subsolidus phase equilibria and ordering in the system ZrO_2–Y_2O_3, Journal of the American Ceramic Society 66 (1983) 23–27.

[10] T. Sato, M. Shimada, Control of the tetragonal-to-monoclinic phase transformation of yttria partially stabilized zirconia in hot water, Journal of Materials Science 20 (1985) 3988–3992.

[11] E.D. Whitney, Kinetics and mechanism of the transition of metastable tetragonal to monoclinic zirconia, Transactions of the Faraday Society 61 (1965) 1991–2000.

[12] W.Z. Zhu, M. Yan, Effect of grain size on the kinetics of isothermal tetragonal to monoclinic transformation in ZrO_2 (2 mol% Y_2O_3) ceramics, Journal of the European Ceramic Society 17 (1997) 1729–1739.

[13] W.Z. Zhu, Effect of cubic phase on the kinetics of the isothermal tetragonal to monoclinic transformation in ZrO_2 (3 mol% Y_2O_3) ceramics, Ceramics International 24 (1998) 35–43.

[14] Y.W. Hsu, K.H. Yang, S.W. Yeah, M.C. Wang, Synthesis and crystallization behavior of 3 mol% yttria stabilized tetragonal zirconia polycrystals (3Y–TZP) nanosized powders prepared using a simple co-precipitation process, Journal of Alloys and Compounds 555 (2013) 82–87.

[15] C.H. Wang, M.C. Wang, J.K. Du, Y.Y. Sie, C.S. Hsi, H.E. Lee, Phase transformation and nanocrystallite growth behavior of 2 mol% yttria–partially stabilized zirconia (2Y–PSZ) powders, Ceramics International 39 (2013) 5165–5174.

[16] B.D. Cullity, Elements of X-ray Diffraction, Addison-Wesley, Reading, MA, 1967, p. 388.

[17] H.S. Liu, T.S. Chin, L.S. Lai, S.Y. Chiu, K.H. Chung, C.S. Chang, Hydroxyapatite synthesized by a simplied hydrothermal method, Ceramics International 23 (1997) 19–25.

[18] C.W. Kuo, Y.H. Shen, S.B. Wen, H.E. Lee, I.M. Hung, H.H. Huang, M.C. Wang, Phase transformation kinetics of 3 mol% yttria partially stabilized zirconia (3Y–PSZ) nanopowders prepared by a non-isothermal process, Ceramics International 37 (2011) 341–347.

[19] G.S. Corman, V.S. Stubican, Phase equilibria and ionic conductivity in the system ZrO_2–Yb_2O_3–Y_2O_3, Journal of the American Ceramic Society 68 (1985) 174–181.

[20] T.S. Sheu, T.Y. Tien, I.W. Chen, Cubic-to tetragonal (t') transformation in zirconia-containing system, Journal of the American Ceramic Society 75 (1992) 1108–1116.

[21] P. Li, I.W. Chen, J.E. Penner-Hahn, Effect of dopants on zirconia stabilization – an X-ray absorption study: I, trivalent dopants, Journal of the American Ceramic Society 77 (1994) 118–128.

[22] N. Igawa, T. Nagasaki, Y. Ishii, K. Noda, H. Ohno, Y. Morii, J.A. Fernandez-Baca, Phase-transformation study of metastable tetragonal zirconia powder, Journal of Materials Science 33 (1998) 4747–4758.

[23] R.W. James, Optical principles of the diffraction of X-rays, The Crystalline State, 2, G. Bell and Sons, London, 1967, p. 34.

[24] M. Cohen, C.M. Wayman, Metallurgical Treatises, Metallurgical Society AIME, Warrendale, PA, 1981, p. 445.

[25] E.S. Machlin, M. Cohen, Burst phenomenon in the martensitic transformation, Transactions of AIME 191 (1951) 746–754.

[26] E.C. Subbaro, H.S. Maiti, K.K. Srivastava, Martensitic transformation in zirconia, Physica Status Solidi A: Applied Research 21 (1974) 9–40.

[27] T.K. Gupta, J.H. Bechtold, R.C. Kuznicki, L.H. Cadoff, B.R. Rossing, Stabilization of tetragonal phase in polycrystalline zirconia, Journal of Materials Science 12 (1971) 2421–2426.

[28] T. Mitsuhashi, M. Ichihara, U. Tatsuke, Characterization and stabilization of metastable tetragonal ZrO_2, Journal of the American Ceramic Society 57 (1974) 97–101.

[29] D.J. Kim, H.J. Huang, D.H. Cho, Phase transformations of Y_2O_3 and Nb_2O_5 doped tetragonal zirconia during low temperature aging in air, Solid State Ionics 80 (1985) 67–75.

[30] R.C. Garvie, The occurrence of metastable tetragonal zirconia as a crystallite size effect, Journal of Physical Chemistry 69 (1965) 1238–1243.

[31] C. Pascual, P.J. Duran, Subsolidus phase equilibria and ordering in the system ZrO_2–Y_2O_3, Journal of the American Ceramic Society 66 (1983) 23–27.

[32] E.D. Whitney, Electrical resistivity and diffusionless phase transformation of zirconia at high temperature and ultrahigh pressure, Journal of the Electrochemical Society 112 (1965) 91–94.

[33] R.P. Denkewicz, K.S. Tenhuisen, J.H. Adair, Hydrothermal crystallization kinetics of m-ZrO_2 and t-ZrO_2, Journal of Materials Research 5 (1990) 2698–2705.

[34] M. Avrami, Kinetics of phase change, Journal of Chemical Physics 7 (1939) 1103–1112.

[35] P. Durán, J. Tartaj, J.F. Fernández, M. Villegas, C. Moure, Crystallisation and sintering behaviour of nanocrystalline Y-TZP powders obtained by seeding-assisted chemical coprecipitation, Ceramics International 25 (1999) 125–135.

[36] A. Marotta, A. Buri, G.L. Valent, Crystallization kinetics of gehlenite glass, Journal of Materials Science (1978) 2483–2486.

[37] J. Chevalier, Low-temperature aging of Y-TZP ceramics, Journal of the American Ceramic Society 82 (1999) 2150–2154.

[38] H. Murakami, H. Ohno, Stability of metastable tetragonal zirconia, Nippon Ceramic Kyokai Gakujustu Ronbunshi 99 (1991) 1234–1239.

[39] W.Z. Zhu, T.C. Lei, Y. Zhou, Time-dependent tetragonal to monoclinic transition in hot-pressed zirconia stabilized with 2 mol% yttria, Journal of Materials Science 28 (1993) 6479–6483.

[40] V. Lughi, D.R. Clarke, Low-temperature transformation kinetics of electron-beam deposited 5 wt% yttria-stabilized zirconia, Acta Materialia 55 (2007) 2049–2055.

[41] Z. Strnad, Glass–Ceramic Materials, Elsevier, Amsterdam, 1986, p. 63–66.

[42] C.W. Kuo, Y.H. Lee, I.M. Hung, M.C. Wang, S.B. Wen, K.Z. Fung, C.J. Shih, Crystallization kinetics and growth mechanism of 8 mol% yttria-stabilized zirconia (8YSZ) nano-powders prepared by a sol–gel process, Journal of Alloys and Compounds 453 (2008) 470–475.

[43] N.L. Wu, T.F. Wu, I.A. Rusakova, Thermodynamic stability of tetragonal zirconia nanocrystallites, Journal of Materials Research 16 (2001) 666–669.